

# Dielectric properties of some low-lead or lead-free perovskite-derived materials: $\text{Na}_{0.5}\text{Bi}_{0.5}\text{TiO}_3\text{-PbZrO}_3$ , $\text{Na}_{0.5}\text{Bi}_{0.5}\text{TiO}_3\text{-BiScO}_3$ and $\text{Na}_{0.5}\text{Bi}_{0.5}\text{TiO}_3\text{-BiFeO}_3$ ceramics

P. Marchet, E. Boucher, V. Dorcet, J.P. Mercurio\*

*Science des Procédés Céramiques et de Traitements de Surface, UMR CNRS 6638, Université de Limoges, Faculté des Sciences et Techniques, 123 Avenue Albert-Thomas, 87060 Limoges Cedex, France*

Available online 10 March 2006

## Abstract

$\text{Na}_{0.5}\text{Bi}_{0.5}\text{TiO}_3$  (NBT) and its modifications are known to be new lead-free ferroelectric materials and are promising for environment friendly devices. The systems under investigation were (i) NBT (trigonal/ferroelectric)– $\text{PbZrO}_3$  (orthorhombic/antiferroelectric); (ii) NBT (trigonal/ferroelectric)– $\text{BiScO}_3$  (trigonal/paraelectric); and (iii) NBT (trigonal/ferroelectric)– $\text{BiFeO}_3$  (trigonal/antiferromagnetic).

The lattice parameters change as expected from the respective ionic radii values. For NBT–PZ, the dielectric permittivity shows a large frequency and temperature dispersion suggesting a relaxor-like behaviour dependent on the thermal annealing of the samples. For NBT–BS, the Curie temperature increases with BS content as well as the diffuseness of the phase transition, connected with the introduced disorder. For NBT–BF, the overall behaviour of the permittivity of NBT is maintained up to 50% BF but anomalies of the permittivity appeared close to 600 °C, which might be connected with the onset of magnetic influence for high BF content.

© 2006 Elsevier Ltd. All rights reserved.

**Keywords:** Perovskites; Dielectric properties

## 1. Introduction

Ferroelectric lead zirconate titanate ceramics (PZT) are extensively used for many industrial purposes due to their high dielectric and electromechanical properties. However, the toxicity of lead oxide and its high vapor pressure during the sintering process results in serious environment problems. As a consequence, it becomes necessary to develop low-lead or lead-free piezoelectric materials with properties close to those of the PZT system.

Sodium bismuth titanate  $\text{Na}_{0.5}\text{Bi}_{0.5}\text{TiO}_3$  (NBT) has attracted considerable attention in the past few decades since it was discovered to be an A-site complex perovskite relaxor by Smolensky et al.<sup>1</sup> NBT has a rhombohedral perovskite-like structure ( $a = 3.89 \text{ \AA}$ ,  $\alpha = 89.6^\circ$ ) with  $\text{Na}^+$  and  $\text{Bi}^{3+}$  ions randomly distributed at the 12-fold cubo-octahedral sites.<sup>2</sup>

NBT is considered to be a good candidate for lead-free piezoelectric ceramic due to its relatively large polariza-

tion ( $38 \mu\text{C}/\text{cm}^2$ ). However, pure NBT has a drawback of high coercive field,  $E_c = 7.3 \text{ kV}/\text{mm}$  and the high conductivity causes problems during the poling process. To improve the properties of NBT, many scientists have added second components to NBT and obtained NBT-based solid solutions, such as NBT– $\text{BaTiO}_3$ , NBT– $\text{PbTiO}_3$ , NBT– $\text{K}_{0.5}\text{B}_{0.5}\text{TiO}_3$ , NBT– $\text{SrTiO}_3$  and NBT– $\text{BiFeO}_3$ .<sup>3–11</sup>

In the search for new compositions, investigation were conducted on systems in which the end members present different crystal structure and/or different electronic properties.

The systems under investigation were (i) NBT (trigonal/ferroelectric)– $\text{PbZrO}_3$  (orthorhombic/antiferroelectric) labelled NBT–PZ; (ii) NBT (trigonal/ferroelectric)– $\text{BiScO}_3$  (trigonal/paraelectric) labelled NBT–BS; and (iii) NBT (trigonal/ferroelectric)– $\text{BiFeO}_3$  (trigonal/antiferromagnetic) labelled NBT–BF.

## 2. Experimental

Solid solutions of the NBT–BT and NBT–ST systems were prepared by high temperature reaction of the corresponding high purity grade oxides or carbonates. After mixing in adequate

\* Corresponding author. Tel.: +33 555 457 477; fax: +33 555 457 270.  
E-mail address: [jpmercurio@unilim.fr](mailto:jpmercurio@unilim.fr) (J.P. Mercurio).

stoichiometric proportions (acetone medium/1 h) and dried at 60 °C, they were calcined at 800–900 °C for 20 h and reheated at 900–1000 °C to ensure complete reaction. Finally, the powders were crushed, using a ball mill, for 15 min in acetone medium.

The sample purity was checked by X-ray diffraction using a  $\theta/2\theta$  Siemens D5000 diffractometer (graphite monochromator, Cu K $\alpha$  radiation). For the lattice parameter measurements, the X-ray diagrams were recorded on an INEL CPS 120 curve detector in a Debye–Scherrer geometry. High-purity silicon was used as internal standard ( $a = 5.43082$  Å). The cell parameters were refined with the “pattern matching” mode of the JANA software.<sup>12</sup>

Disk-shaped ceramics (12 mm diameter, 1.5 mm thickness) with densities close to 95% of theoretical were obtained by conventional sintering the above-prepared powders (cold pressed at 100 MPa) at 1050–1200 °C, depending on the composition. After polishing, they were coated with a silver paste fired at 600 °C and aged overnight at 100 °C. Low-frequency dielectric measurements were carried out between room temperature and 700 °C (heating/cooling rate, 1 °C min<sup>-1</sup>) at several frequencies from 100 Hz to 1 MHz using a HP 4194A impedance analyser.

### 3. Results and discussion

#### 3.1. Structural characterization

The solid-state mutual miscibilities are generally strongly dependent on the crystal symmetry as well as on the size of the cations in their respective coordination numbers. Here lead ( $r_{\text{Pb}^{2+}_{[12]}} = 1.49$  Å) in PZ and bismuth ( $r_{\text{Bi}^{3+}_{[12]}} = 1.30$  Å est.) in both BS and BF are likely to substitute for [Na,Bi] ( $r_{[\text{Na,Bi}]^{2+}_{[12]}} = 1.35$  Å est.) in the 12-fold coordination site of the perovskite whereas zirconium ( $r_{\text{Zr}^{4+}_{[6]}} = 0.72$  Å), scandium ( $r_{\text{Sc}^{3+}_{[6]}} = 0.745$  Å) and iron ( $r_{\text{Fe}^{3+}_{[6]}} = 0.645$  Å) will occupy the six-fold coordination sites.<sup>13</sup> The solubility limits and the unit cell symmetry of the solid solutions have been derived from room temperature X-ray diffraction patterns. The main features are given in Fig. 1. PZ and BF are fully miscible in NBT. The solubility of BS was estimated to be about 25 mol.% BS, as an extra phase (sillenite-type Bi<sub>12</sub>Ti<sub>20</sub>) always appeared for richer compositions. In addition, whereas the NBT–BS solid solutions keep the trigonal symmetry in the whole composition range, the NBT–PZ solid solutions exhibit various symmetries: they are trigonal for NBT-rich ( $\leq 20$  mol.% PZ) and orthorhombic

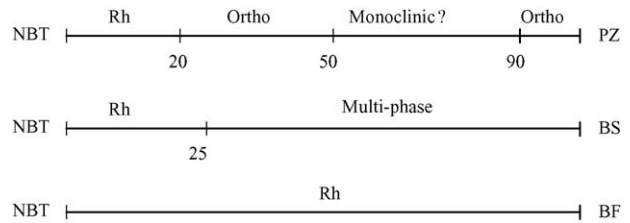


Fig. 1. Symmetry of the NBT–PZ, NBT–BS and NBT–BF solid solutions.

for 20 mol.%  $\leq$  [PZ]  $\leq$  60 mol.% PZ and PZ-rich ( $\geq 90$  mol.% PZ) compositions. It seems that for compositions in the range 60–90 mol.% PZ, the symmetry would be lower, apparently monoclinic.

The variations of the lattice parameters are given in Fig. 2. The overall evolutions are consistent with the modifications of the mean ionic radii induced by the respective substitutions. As the substitutions increase, the lattice parameters increase with the following rates: 6.7% for PZ, 3.6% for BS and 1.9% for BF. When PZ is substituted for NBT, Pb<sup>2+</sup> and Zr<sup>4+</sup> contribute to the increase of the cell dimension as they are significantly larger than [Na,Bi]<sup>2+</sup> and Ti<sup>4+</sup>, respectively. In the two other cases, Bi<sup>3+</sup> is likely to substitute for Na<sup>+</sup> in the 12-fold coordinated site. As its ionic radius is smaller than that of Na<sup>+</sup>, it does not have any influence on the lattice parameters, the increase of which is mainly due to Sc<sup>3+</sup> and Fe<sup>3+</sup>. As Sc<sup>3+</sup> is much larger than Fe<sup>3+</sup>, the observed increase rate behaves as expected.

#### 3.2. Dielectric properties

Cationic substitutions in ferroelectric perovskites like BaTiO<sub>3</sub> or PbTiO<sub>3</sub> are known to influence significantly the dielectric properties, especially the values of the permittivity and the Curie temperature. In some cases, the disorder induced by the substitution could be at the origin of the onset of relaxation process. Such phenomena have already been observed for some modified NBT solid solutions, e.g. NBT–BT, NBT–PT, NBT–KBT, NBT–ST. They strongly depend on the nature of the substituting cations. In the present work, as the substitutions involve both A and B sites and the end members PZ, BS and BF have different dielectric character (PZ antiferroelectric, BS paraelectric, BF ferroelectric/antiferromagnetic), the substituted materials would behave quite differently from one another.

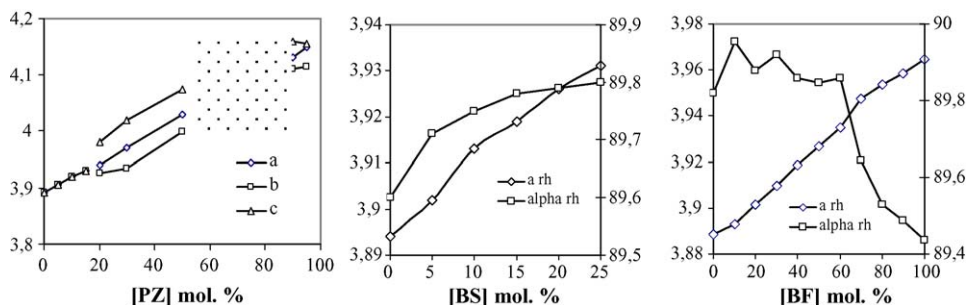


Fig. 2. Lattice parameters (Å) and angles (°) of the NBT–PZ, NBT–BS and NBT–BF solid solutions vs. composition (for NBT–PZ, the shadow region indicates possible monoclinic symmetry, see text).

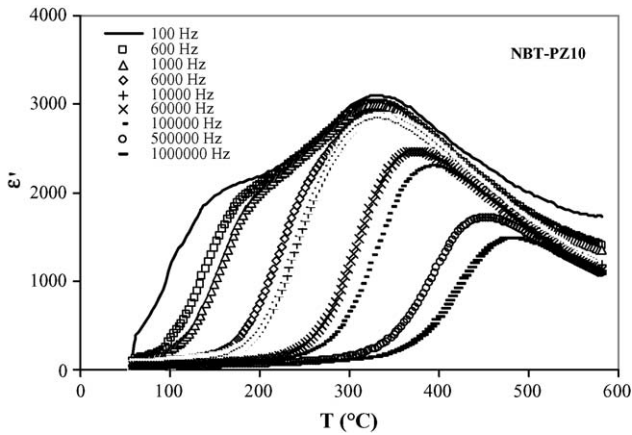


Fig. 3. Variation of the permittivity of NBT–PZ10% as a function of temperature at several frequencies.

The permittivities and dielectric losses of ceramic materials were measured for the three systems from room temperature to 700–800 °C between 10<sup>2</sup> and 10<sup>6</sup> Hz. For sake of clarity, only the results of the permittivity of some selected compositions will be given.

### 3.2.1. NBT–PZ system

The solid solutions are made from a ferroelectric (NBT) and an antiferroelectric (PZ) material. For low PZ content, the variations of the permittivity do not strongly change with respect to NBT. Figs. 3 and 4 show the results obtained for NBT–PZ10 and NBT–PZ20 as received from sintering; the low temperature, frequency-dependent hump is retained up to 20 mol.% PZ as well as the maximum assigned to the Curie temperature. For compositions richer than 20 mol.% PZ (not given here), the hump has disappeared and only the local maximum remains. One can observe that the maximum at about 320 °C is frequency-independent at low frequency but is strongly shifted towards the high temperature side and the value of the maximum permittivity decreases as the measuring frequency increases above 1 kHz. This is a significant kind of relaxation process. As it appears in the range 10<sup>3</sup>–10<sup>6</sup> Hz and at high temperature (>300 °C), it could be connected with macrostructural defects, grain boundary or

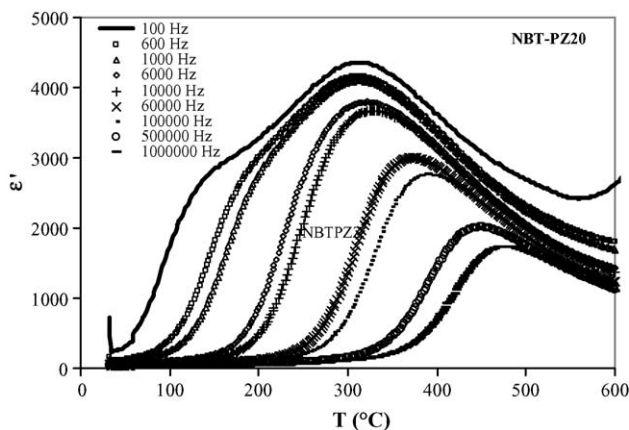


Fig. 4. Variation of the permittivity of NBT–PZ20% as a function of temperature at several frequencies.

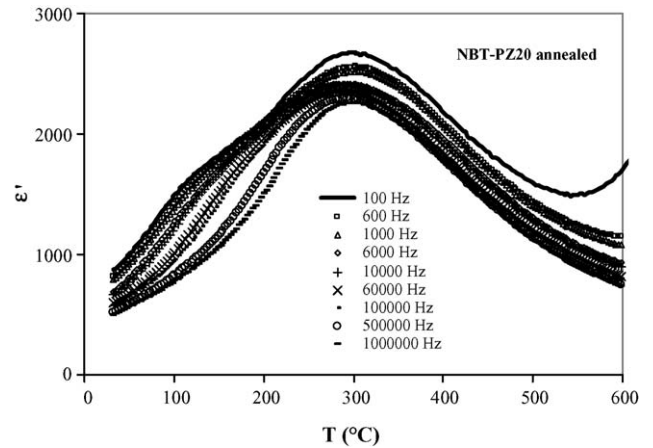


Fig. 5. Variation of the permittivity of NBT–PZ20% as a function of temperature at several frequencies after annealing.

space charge effects. This assumption is supported by the results obtained for the same NBT–PZ20 sample annealed at 700 °C (Fig. 5): the local maximum is now frequency-independent and the aforementioned relaxation is no longer visible. Such behaviour was observed for all compositions.

### 3.2.2. NBT–BS system

Fig. 6 shows the temperature dependence of the permittivity of NBT–BS ceramics. A substantial decrease of the dielectric maximum  $\epsilon_{r \max}$  occurs with increasing BS content. In addition, the Curie point  $T_C$  is shifted towards higher temperatures, from 340 °C (NBT) to 385 °C (75NBT–25BS) and the transition at  $T_C$  becomes more and more diffuse. The diffuseness of the ferroelectric/paraelectric transition can be quantified by the factor  $\delta$ , calculated from the following relation:

$$\frac{1}{\epsilon_r} = \frac{1}{\epsilon_{r \max}} + \frac{(T - T_C)^2}{2\epsilon_{r \max}\delta^2} \quad (1)$$

where  $\epsilon_{r \max}$  is the maximum permittivity and  $T_C$  the Curie point.<sup>14</sup> The values of  $\delta$  obtained from the slope of plots of

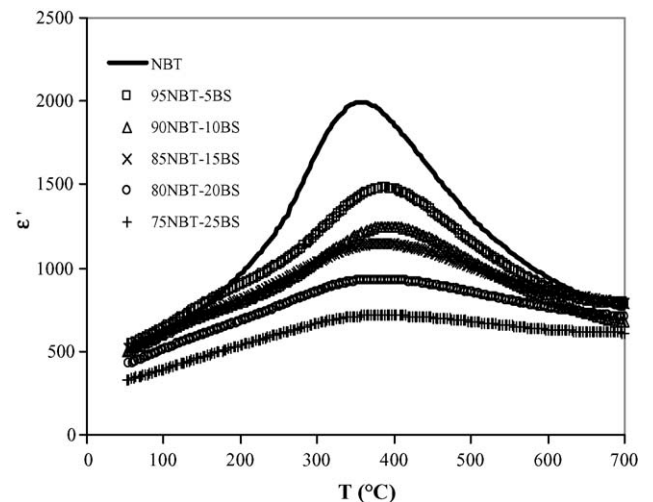


Fig. 6. Variation of the permittivity of several NBT–BS solid solutions as a function of temperature at 1 kHz.

Table 1

Curie point ( $T_C$ ), permittivity maximum  $\epsilon_{r\max}$  and diffusive factor ( $\delta$ ) of the various NBT–BS compositions

Mol. % BS	0	5	10	15	20	25
$T_C$ (°C)	340	383	397	385	386	385
$\epsilon_{r\max}$	2125	1510	1270	1150	940	720
$\delta$ (°C)	110	133	158	209	229	255

$1/\epsilon$  versus  $(T - T_C)^2$ , are given in Table 1. The substitution of Sc for Ti in the B-site of the perovkite structure is the main factor that induces some disorder in the cationic octahedral sublattice and then produces an increase of the diffuseness of the structural phase transition at  $T_C$ .

The variation of the permittivity as a function of temperature at several frequencies shows similarities with that of the previous system as shown in Fig. 7 for the NBT–BS10 ceramics, but the relaxation is much less pronounced.

### 3.2.3. NBT–BF system

This system behaves in a different way with respect to the two previous ones. Two ranges of compositions can be distinguished. For BF content  $\leq 50$  mol.%, the overall behaviour of the permittivity is similar to that observed for low substituted NBT (Fig. 8 top) but the local maximum is shifted towards higher temperatures as the BF content increases. This can be connected with the high Curie temperature of  $\text{BiFeO}_3$ . For BF content  $> 50$  mol.%, the maximum of the permittivity has disappeared, but an additional maximum occurs at high temperatures between 600 and 750 °C (Fig. 8 bottom). The substitution of  $\text{Fe}^{3+}$  for  $\text{Ti}^{4+}$  has an influence not only on the structural characteristics but also on the electromagnetic behaviour as  $\text{Fe}^{3+}$  has a  $d^5$  electronic configuration, with a finite magnetic moment (in contrast,  $\text{Zr}^{4+}$  and  $\text{Sc}^{3+}$  are spherical ions with non-magnetic  $d^0$  configuration). It is therefore reasonable to infer that this anomalous behaviour would be somewhat connected with the magnetic character of the BF-rich materials. In addition, as the ceramics become more

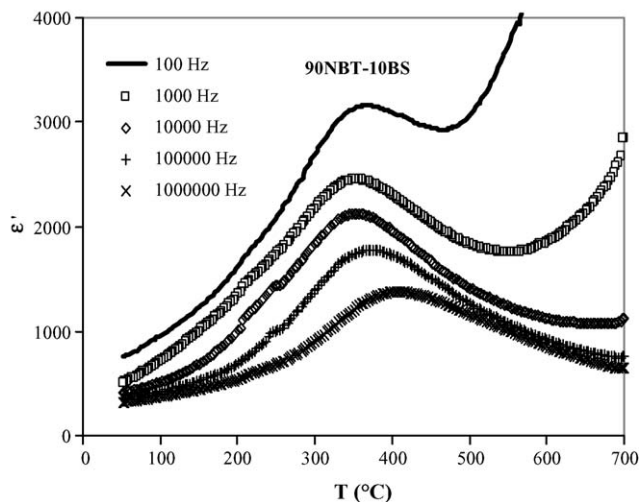


Fig. 7. Variation of the permittivity of the NBT–BS10% solid solution as a function of temperature at several frequencies.

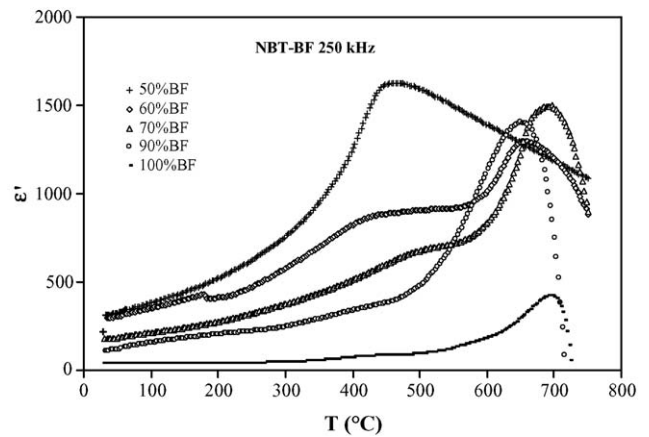
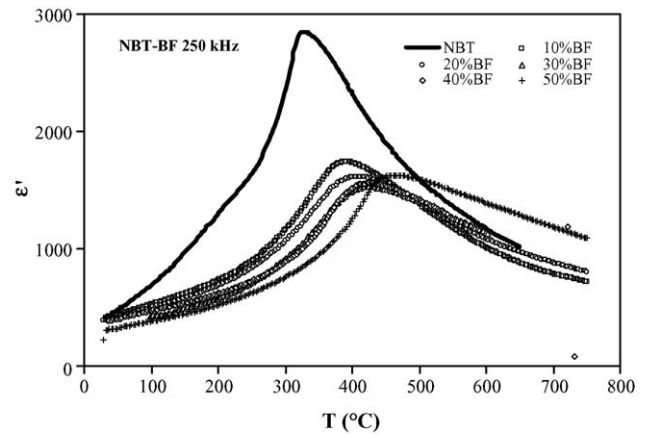


Fig. 8. Variation of the permittivity of the NBT–BF solid solutions as a function of temperature at 250 kHz.

conductive for high BF contents, one cannot neglect the presence of mixed-valence ( $\text{Fe}^{2+}/\text{Fe}^{3+}$ ) cations, which might influence the high dielectric behaviour. Further investigations about this problem are now in progress.

## 4. Conclusion

The systems NBT– $\text{PbZrO}_3$  (orthorhombic/antiferroelectric), NBT (trigonal/ferroelectric)– $\text{BiScO}_3$  (trigonal/paraelectric) and NBT (trigonal/ferroelectric)– $\text{BiFeO}_3$  (trigonal/antiferromagnetic) were investigated from structural and dielectric points of view. The end members are fully miscible except  $\text{BiScO}_3$  for which the solubility is limited to 25 mol.% BS. The evolutions of the lattice parameters of the solid solutions are connected to those of the average ionic radii. The dielectric properties are similar to that of NBT for low levels of substitution and the phase transition to the paraelectric state is more and more diffuse as the substitution increases. In the case of BF-substituted materials an up-to-now unexplained anomaly of the permittivity occurs at high temperature, which might be connected with both conductivity and magnetism.

## References

- Smolenski, G. A., Isupov, V. A., Agranovskaya, A. I. and Krainik, N. N., *Sov. Phys. Solid State*, 1961, 2, 2651.

2. Jones, G. O. and Thomas, P. A., *Acta crystallogr.*, 2002, **B58**, 168.
3. Takenaka, T., Sakata, K. and Toda, K., *Ferroelectrics*, 1990, **106**, 375.
4. Takenaka, T., Okuda, T. and Takegahara, K., *Ferroelectrics*, 1997, **196**, 175.
5. Nagata, H. and Takenaka, T., *Jpn. J. Appl. Phys.*, 1998, **37(9B)**, 5311.
6. Herabut, A. and Safari, A., *J. Am. Ceram. Soc.*, 1997, **80**, 2954.
7. Wang, T. B., Gao, M., Wang, L. E., Lu, Y. K. and Zhou, D. P., *J. Inorg. Mater.*, 1997, **2**, 223.
8. Kuharuangrong, S. and Schulze, W., *J. Am. Ceram. Soc.*, 1996, **79**, 1273.
9. Sakata, K. and Masuda, Y., *Ferroelectrics*, 1974, **7**, 347.
10. Saïd, S. and Mercurio, J.-P., *J. Eur. Ceram. Soc.*, 2001, **21**, 1333.
11. Gomah-Petry, J. R., Salak, A. N., Marchet, P., Ferreira, V. M. and Mercurio, J.-P., *Phys. Status Solidi B*, 2004, **241(8)**, 1949.
12. Petricek, V., Dusek, M. and Palatinus, L., *JANA 2000: The Crystallographic Computing System*. Institute of Physics, Praha, Czech Republic.
13. Shannon, R. D. and Prewitt, C. T., *Acta Crystallogr.*, 1970, **B26**, 1046.
14. Xia, F. and Yao, X., *J. Mater. Sci.*, 1999, **34**, 3341.